



Since January 2020 Elsevier has created a COVID-19 resource centre with free information in English and Mandarin on the novel coronavirus COVID-19. The COVID-19 resource centre is hosted on Elsevier Connect, the company's public news and information website.

Elsevier hereby grants permission to make all its COVID-19-related research that is available on the COVID-19 resource centre - including this research content - immediately available in PubMed Central and other publicly funded repositories, such as the WHO COVID database with rights for unrestricted research re-use and analyses in any form or by any means with acknowledgement of the original source. These permissions are granted for free by Elsevier for as long as the COVID-19 resource centre remains active.



Short communication

## An epidemiological model for SARS-CoV-2

L.H.A. Monteiro<sup>a,b</sup><sup>a</sup> Universidade Presbiteriana Mackenzie, Escola de Engenharia, Rua da Consolação, n.896, São Paulo, 01302-907, SP, Brazil<sup>b</sup> Universidade de São Paulo, Escola Politécnica, São Paulo, SP, Brazil

## ARTICLE INFO

## Keywords:

Basic reproduction number  
 COVID-19  
 Dynamical systems  
 Epidemic model  
 SARS-CoV-2

## ABSTRACT

The spread of SARS-CoV-2 (severe acute respiratory syndrome coronavirus 2) is here investigated from an epidemic model considering four pathways of person-to-person transmission. These pathways represent the propagation of this novel coronavirus by asymptomatic and symptomatic infected individuals. In this work, analytical expressions for the disease-free and endemic steady-states are derived. Also, the conditions for eradication of this contagious disease are determined. By taking into account realistic parameter values, the proposed model shows an oscillatory convergence to the endemic steady-state, which means the occurrence of a sequence of peaks in the number of sick individuals as time passes. These results are discussed from a public health standpoint.

## 1. Introduction

The ongoing pandemic of coronavirus disease 2019 (COVID-19) has been responsible for countless deaths, many of them due to the lack of adequate medical treatment, even in developed countries (Singhal, 2020; Velavan and Meyer, 2020). Two main features of this disease, which is caused by the severe acute respiratory syndrome coronavirus 2 (SARS-CoV-2), are (Lai et al., 2020; Mizumoto et al., 2020; Singhal, 2020): asymptomatic carriers can transmit the pathogen and notable interindividual variation in the course of infection (from absence of clinical manifestations to severe pneumonia and multi-organ dysfunction, requiring intensive care).

Theoretical investigations on the spread of contagious infections can support the decision-making processes by public health authorities (Ferraz and Monteiro, 2019; Fitch, 2015; Kretzschmar, 2019; Pennekamp et al., 2017; Schimit and Monteiro, 2010; Tang et al., 2020). Hence, despite its recent emergence, some aspects of the outbreak of the novel coronavirus were already theoretically examined. For instance, epidemic models were conceived to evaluate the impact of mass media (Zhou et al., 2020) and screening programs (Gostic et al., 2020) on reducing the propagation.

Assume that each individual is in one of four health states: susceptible ( $S$ ), asymptomatic infected ( $A$ ), symptomatic infected ( $I$ ), or recovered ( $R$ ). Asymptomatic means without symptoms; symptomatic means with symptoms, varying from mild to critical. The novelty of the model proposed here is to decompose the contagion in the following four pathways:  $S + A \xrightarrow{a_1} 2A$ ,  $S + A \xrightarrow{a_2} I + A$ ,  $S + I \xrightarrow{a_1} A + I$ , and  $S + I \xrightarrow{a_2} 2I$ . These state transitions are characterized by the rate

constants  $\alpha_1$ ,  $\alpha_2$ ,  $a_1$ , and  $a_2$ . In works found in the literature (Gostic et al., 2020; Yang and Wang, 2020; Zhou et al., 2020), different transmission pathways of COVID-19 have been considered.

This paper is organized as follows. In Section 2, a deterministic compartmental model written in terms of differential equations is introduced and analyzed. Recall that a compartment is a homogeneous subpopulation. In Section 3, numerical simulations are presented to illustrate the spread of the infectious agent. In Section 4, the possible relevance of this study is stressed.

## 2. The SAIR model

Let  $S(t)$ ,  $A(t)$ ,  $I(t)$ , and  $R(t)$  be the numbers of  $S$ ,  $A$ ,  $I$ , and  $R$ -individuals in a given geographic region at the instant  $t$ , respectively. By taking into consideration the homogeneous mixing assumption (Turnes and Monteiro, 2014), the proposed model is described by the following set of first-order differential equations:

$$\frac{dS(t)}{dt} = -\alpha S(t)A(t) - aS(t)I(t) + \gamma A(t) + cI(t) + dR(t) \quad (1)$$

$$\frac{dA(t)}{dt} = \alpha_1 S(t)A(t) + a_1 S(t)I(t) - \beta A(t) - \gamma A(t) \quad (2)$$

$$\frac{dI(t)}{dt} = \alpha_2 S(t)A(t) + a_2 S(t)I(t) - bI(t) - cI(t) \quad (3)$$

$$\frac{dR(t)}{dt} = \beta A(t) + bI(t) - dR(t) \quad (4)$$

The nine parameters  $\alpha_1$ ,  $\alpha_2$ ,  $\beta$ ,  $\gamma$ ,  $a_1$ ,  $a_2$ ,  $b$ ,  $c$ , and  $d$  are positive numbers.

E-mail addresses: [luizm@mackenzie.br](mailto:luizm@mackenzie.br), [luizm@usp.br](mailto:luizm@usp.br).

<https://doi.org/10.1016/j.ecocom.2020.100836>

Received 5 April 2020; Received in revised form 8 May 2020; Accepted 18 May 2020

Available online 29 May 2020

1476-945X/ © 2020 Elsevier B.V. All rights reserved.

The rate constants  $\alpha_1$  and  $a_1$  respectively express the transmission by  $A$  and  $I$ -individuals to  $S$ -individuals leading to  $A$ -individuals;  $\alpha_2$  and  $a_2$  respectively express the transmission by  $A$  and  $I$ -individuals to  $S$ -individuals leading to  $I$ -individuals. Thus, the rate constants  $\alpha = \alpha_1 + \alpha_2$  and  $a = a_1 + a_2$  are related to the infections caused by  $A$  and  $I$  individuals, respectively. Also,  $\beta$  and  $b$  are the recovery rate constants of  $A$  and  $I$ -individuals, respectively;  $\gamma$  and  $c$  are the death rate constants of  $A$  and  $I$ -individuals, respectively; and  $d$  is the death rate constant of  $R$ -individuals. In addition,  $R$ -individuals are supposed to be fully protected from reinfections. If this is not true, then  $d$  also includes the immunity-loss rate constant.

Note that  $dS(t)/dt + dA(t)/dt + dI(t)/dt + dR(t)/dt = 0$ , because the deaths of  $A$ ,  $I$ , and  $R$ -individuals are balanced by the births of  $S$ -individuals. Therefore,  $S(t) + A(t) + I(t) + R(t) = N$ ; that is, the total number of individuals  $N$  remains constant. Since  $R(t) = N - S(t) - A(t) - I(t)$ , the model can be rewritten as:

$$\frac{dS}{dt} = -\alpha SA - aSI + \gamma A + cI + d(N - S - A - I) \tag{5}$$

$$\frac{dA}{dt} = \alpha_1 SA + a_1 SI - \beta A - \gamma A \tag{6}$$

$$\frac{dI}{dt} = \alpha_2 SA + a_2 SI - bI - cI \tag{7}$$

This third-order system is analyzed from a dynamical systems theory perspective (Guckenheimer and Holmes, 2002). A stationary solution  $(S^*, A^*, I^*)$ , corresponding to an equilibrium point in the state space  $S \times A \times I$ , is obtained from  $dS/dt = 0$ ,  $dA/dt = 0$ , and  $dI/dt = 0$ . In this model, there are a disease-free stationary solution given by:

$$(S_1^*, A_1^*, I_1^*) = (N, 0, 0) \tag{8}$$

and an endemic stationary solution given by:

$$(S_2^*, A_2^*, I_2^*) = \left( \frac{-n + \sqrt{n^2 + 4mp}}{2m}, \frac{d(N - S_2^*)q}{c - d + aS_2^* + (\alpha S_2^*/q)}, qA_2^* \right) \tag{9}$$

with:

$$m = a_1\alpha_2 - a_2\alpha_1 \tag{10}$$

$$n = (\beta + \gamma)a_2 + (b + c)\alpha_1 \tag{11}$$

$$p = (\beta + \gamma)(b + c) \tag{12}$$

$$q = \frac{\beta + \gamma - \alpha_1 S_2^*}{a_1 S_2^*} \tag{13}$$

If  $m = 0$ , then  $S_2^* = p/n$ .

The local stability of an equilibrium point can be inferred from the eigenvalues of the Jacobian matrix  $J$ , which is obtained from the linearization of the set of non-linear differential equations around such a point. Let  $\lambda$  be the eigenvalues of  $J$ , which are determined from  $\det(J - \lambda I) = 0$  ( $I$  is the identity matrix). The Hartman–Grobman theorem (Guckenheimer and Holmes, 2002) says that an equilibrium point is locally asymptotically stable if all its eigenvalues have negative real parts; if at least one eigenvalue has positive real part, then this point is unstable.

Consider the parameters  $\rho_1$  and  $\rho_2$  defined as:

$$\rho_1 = \frac{(\alpha_1 + \alpha_2)N}{\beta + \gamma + b + c} \tag{14}$$

$$\rho_2 = \frac{a_1\alpha_2 N^2}{[\alpha_1 N - (\beta + \gamma)][a_2 N - (b + c)]} \tag{15}$$

Stability analysis of the SAIR model reveals that its disease-free solution is asymptotically stable if  $\rho_1 < 1$  and  $\rho_2 < 1$ , and it is unstable if  $\rho_1 > 1$  and/or  $\rho_2 > 1$ .

In epidemiology, the basic reproduction number  $R_0$  is defined as the average number of secondary infections caused by a single infectious

individual inserted into a completely susceptible population (Anderson and May, 1992). Therefore, if  $R_0 > 1$ , the corresponding pathogen can invade and/or chronically persist in the host population; if  $R_0 < 1$ , it cannot invade and/or it will be naturally eradicated. A formula for  $R_0$  can be derived from a method based on the next generation matrix  $FV^{-1}$  (Diekmann et al., 2010; van den Driessche, 2017). In this method,  $R_0$  is the spectral radius of  $FV^{-1}$ , in which  $F$  is a matrix related to the appearance of new infections in the infected compartments (which are  $A$  and  $I$ ) and  $V$  is a matrix related to the other transitions occurring in these (two) infected compartments. For the proposed model:

$$R_0 = |\theta + \sqrt{\theta^2 - \sigma}| \tag{16}$$

with  $\theta = nN/(2p)$  and  $\sigma = -mN^2/p$ . If  $\alpha_1 = \alpha_2 = 0$  (no transmission by asymptomatic carriers), then  $R_0 = a_2N/(b + c)$ , which is a mathematical expression already found in other studies (Ferraz and Monteiro, 2019; Monteiro et al., 2006).

Therefore, the disease eradication requires  $\rho_1 < 1$  and  $\rho_2 < 1$  (from the Jacobian matrix  $J$ ); alternatively,  $R_0 < 1$  (from the next generation matrix  $FV^{-1}$ ).

### 3. Simulation results

The SAIR model was numerically solved by using the 4th-order RungeKutta integration method with integration time step of 0.01. In the simulations,  $N = 1$ ; therefore, the variables of the model represent normalized amounts of  $S$ ,  $A$ ,  $I$ , and  $R$ -individuals. The initial condition is  $A(0) + I(0) = 0.0001$ , and  $R(0) = 0$ . This initial condition means no pre-existing immunity in humans and introduction of the virus by 0.01% of infected individuals. The time  $t$  is measured in days.

Initially, assume that recovery from infection induces long-lasting immunity. Assume also that  $A$  and  $R$ -individuals have equal death rates; thus, if their average life expectancy is 80 years, then  $\gamma = d = [1/(365 \times 80)]\text{day}^{-1}$ . The death rate of  $I$ -individuals is simplistically taken as  $c = [3/(100 \times 20)]\text{day}^{-1}$  (since 3% of  $I$ -individuals dies 20 days after being sick (Wu et al., 2020)). Also, the infectious periods for  $A$  and  $I$ -individuals are taken as 10 days (Hu et al., 2020) and 15 days (Singhal, 2020) (including an incubation period of 5 days (Singhal, 2020)); thus,  $\beta = (1/10)\text{day}^{-1}$  and  $b = (1/15)\text{day}^{-1}$ . The choices of the contagion rate constants  $\alpha_1$ ,  $\alpha_2$ ,  $a_1$ , and  $a_2$  should give  $R_0 \approx 2 - 6$  (Gostic et al., 2020; Singhal, 2020; Tang et al., 2020; Wu et al., 2020) and  $q \approx 0.25 - 9$ . The reason for this range of  $q$  is the following. The whole infected compartment in steady state is given by the sum of the asymptomatic fraction  $f_a$  and the symptomatic fraction  $f_i$ , that is,  $f_a + f_i = 1$ , with  $f_a = A_2^*/(A_2^* + I_2^*)$  and  $f_i = I_2^*/(A_2^* + I_2^*)$ . If  $q = I_2^*/A_2^* = f_i/f_a$ , then  $q = (1 - f_a)/f_a$ . The infected compartment is composed from 10% of  $A$ -individuals (Mizumoto et al., 2020; Singhal, 2020) to 80% of  $A$ -individuals (Day, 2020a; 2020b). Therefore, if  $f_a = 0.1$ , then  $q = 9$ ; if  $f_a = 0.8$ , then  $q = 0.25$ .

Fig. 1 exhibits the time evolution of  $S(t)$  (green line),  $A(t)$  (black line),  $I(t)$  (red line), and  $R(t)$  (blue line) for  $a_1 = 0.01$ ,  $a_2 = 0.1$ ,  $\alpha_1 = 0.2$ , and  $\alpha_2 = 0.5$ . With these choices,  $\rho_1 \approx 1.8 > 1$ ,  $\rho_2 \approx 1.6 > 1$ , and  $R_0 \approx 2.6 > 1$ ; hence, the disease-free solution is unstable. Note that the behavior observed in the first 200 days can suggest that the disease would tend to naturally disappear. However, by increasing the simulation time interval, as shown in Fig. 2, there occurs an oscillatory convergence to the endemic steady-state, given by  $S(t) \rightarrow S_2^* \approx 0.38$ ,  $A(t) \rightarrow A_2^* \approx 0.00004$ , and  $I(t) \rightarrow I_2^* \approx 0.00025$ , with  $q = I_2^*/A_2^* \approx 6.3$ . Obviously,  $R(t) \rightarrow R_2^* = 1 - (S_2^* + A_2^* + I_2^*) \approx 0.62$ . In this simulation,  $A_2^* + I_2^* \approx 0.03\%$ . This is the percentage of infected individuals found in steady state. Fig. 3 presents only  $I(t)$  to better visualize its time evolution. The first peak occurs at  $t_{peak} = 72$ . At this instant,  $I(t_{peak}) \approx 0.24$ ; that is, about 1/4 of the whole population would be symptomatically infected. In this simulation, this peak is reached from an initial condition in which 0.01% of the individuals are infected. The lower the

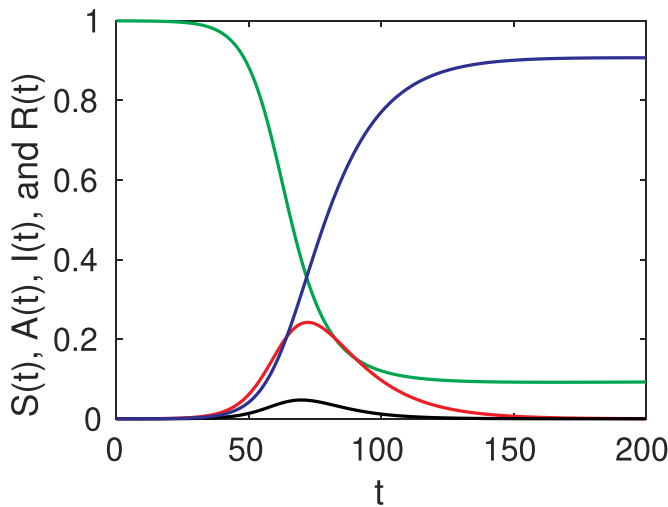


**Fig. 1.** Time evolutions of  $S(t)$  (green line),  $A(t)$  (black line),  $I(t)$  (red line), and  $R(t)$  (blue line) from  $S(0) = 99.99\%$ ,  $A(0) = 0.001\%$ ,  $I(0) = 0.009\%$ , and  $R(0) = 0\%$  obtained from the numerical integration of Eqs. (1)–(4) for  $N = 1$  and  $0 \leq t \leq 200$ . In this computer simulation, the parameter values are  $a_1 = 0.01$ ,  $a_2 = 0.1$ ,  $\alpha_1 = 0.2$ ,  $\alpha_2 = 0.5$ ,  $b = 1/15$ ,  $\beta = 1/10$ ,  $c = 3/(100 \times 20)$ , and  $\gamma = d = 1/(365 \times 80)$ . Observe that, apparently, the disease would tend to naturally disappear. (For interpretation of the references to color in this figure legend, the reader is referred to the web version of this article.)

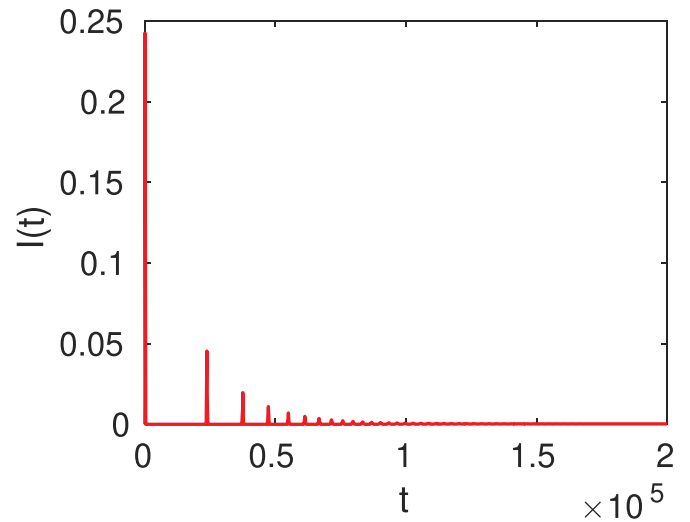


**Fig. 3.** Time evolution of  $I(t)$  presented in Fig. 2.

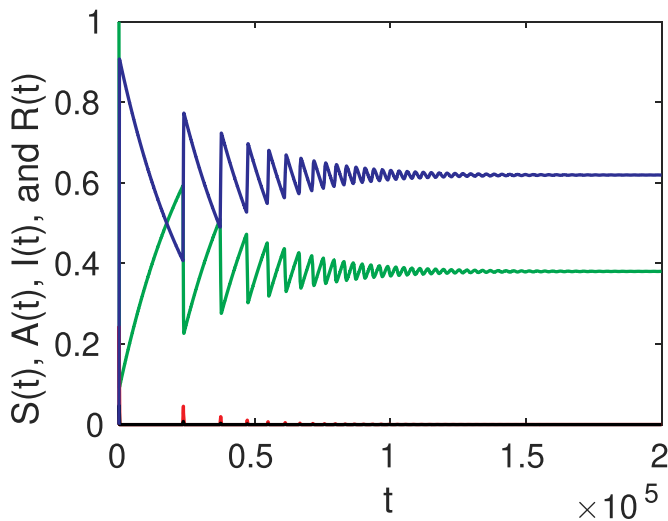


**Fig. 2.** Time evolutions of  $S(t)$  (green line),  $A(t)$  (black line),  $I(t)$  (red line), and  $R(t)$  (blue line) by using the same parameter values as employed in Fig. 1 and a larger time interval of the simulation. After an oscillatory transient, the system reaches an endemic steady-state given by  $S_2^* \simeq 0.38$ ,  $A_2^* \simeq 0.000040$ ,  $I_2^* \simeq 0.00025$ , and  $R_2^* \simeq 0.62$ . Hence, the disease persists. (For interpretation of the references to color in this figure legend, the reader is referred to the web version of this article.)

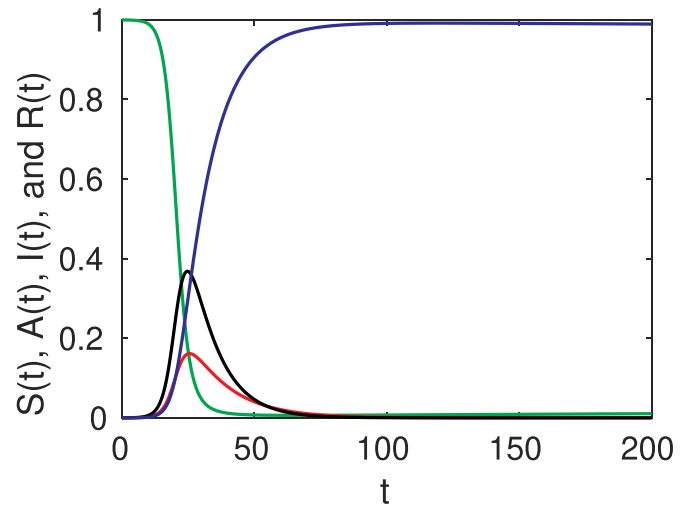


**Fig. 4.** Time evolutions of  $S(t)$  (green line),  $A(t)$  (black line),  $I(t)$  (red line), and  $R(t)$  (blue line) from  $S(0) = 99.99\%$ ,  $A(0) = 0.009\%$ ,  $I(0) = 0.001\%$ , and  $R(0) = 0\%$  obtained from the numerical integration of Eqs. (1)–(4) for  $N = 1$  and  $0 \leq t \leq 200$ . In this simulation, the parameter values are  $a_1 = 0.1$ ,  $a_2 = 0.01$ ,  $\alpha_1 = 0.5$ ,  $\alpha_2 = 0.2$ ,  $b = 1/15$ ,  $\beta = 1/10$ ,  $c = 3/(100 \times 20)$ , and  $\gamma = d = 1/(365 \times 80)$ . As in Fig. 1, the disease apparently tends to disappear. (For interpretation of the references to color in this figure legend, the reader is referred to the web version of this article.)

initial number of infected individuals, the later the first peak occurs. The initial condition, however, does not affect the steady state reached by the system as  $t \rightarrow \infty$ .

For  $a_1 = 0.1$ ,  $a_2 = 0.01$ ,  $\alpha_1 = 0.5$ , and  $\alpha_2 = 0.2$  (that is, by switching the values of the contagion parameters used in Figs. 1–3), then  $S(t) \rightarrow S_2^* \simeq 0.18$ ,  $R(t) \rightarrow R_2^* \simeq 0.82$ ,  $A(t) \rightarrow A_2^* \simeq 0.00020$ , and  $I(t) \rightarrow I_2^* \simeq 0.00011$ , with  $q = I_2^*/A_2^* \simeq 0.54$ . Also,  $\rho_1 \simeq 3.0$ ,  $\rho_2 \simeq -0.9$ , and  $R_0 \simeq 5.5$ . The first peak, with  $I(t_{peak}) \simeq 0.16$ , occurs at  $t_{peak} = 26$ . Fig. 4 presents the time evolution of  $S(t)$ ,  $A(t)$ ,  $I(t)$ , and  $R(t)$  in the first 200 days. Observe that, in Fig. 1 (with  $a_1 < a_2$  and  $\alpha_1 < \alpha_2$ ),  $I(t) > A(t)$ ; in Fig. 4 (with  $a_1 > a_2$  and  $\alpha_1 > \alpha_2$ ),  $I(t) < A(t)$ . Figs. 5 and 6 show a transient with peaks in  $A(t)$  and  $I(t)$  separated by

quiescent periods, as observed in Figs. 2 and 3.

For  $a_1 = 0.005$ ,  $a_2 = 0.06$ ,  $\alpha_1 = 0.01$ , and  $\alpha_2 = 0.02$  (which are smaller numbers than those used in Figs. 1–6), a numerical simulation shows that  $S(t) \rightarrow S_1^* = 1$ ,  $A(t) \rightarrow A_1^* = 0$ , and  $I(t) \rightarrow I_1^* = 0$  (obviously,  $R(t) \rightarrow R_1^* = 0$ ). For these parameter values,  $\rho_1 = 0.42 < 1$ ,  $\rho_2 = 0.14 < 1$ , and  $R_0 = 0.90 < 1$ ; consequently, there is a convergence to the disease-free steady-state. A reduction in the transmission parameters can occur by imposing isolation, lockdown, quarantine, travel restrictions.

A relevant observation: if this infection does not confer long-term immunity, then the value of  $d$  should be higher. Fig. 7 presents the dynamical behavior obtained in a simulation with  $d = [1/(365 \times 80)] + (1/365)$ ; that is, the acquired immunity lasts for one year. The other parameter values are the same as used in Figs. 1–3. In this case,  $S(t) \rightarrow S_2^* \simeq 0.38$ ,  $A(t) \rightarrow A_2^* \simeq 0.003$ ,  $I(t) \rightarrow I_2^* \simeq 0.021$ ,  $R(t) \rightarrow R_2^* \simeq 0.60$ . Also,  $\rho_1 \simeq 1.8$ ,  $\rho_2 \simeq 1.6$ ,  $R_0 \simeq 2.6$ , and  $q \simeq 6.3$ . Observe that the convergence is also oscillatory to the endemic steady-

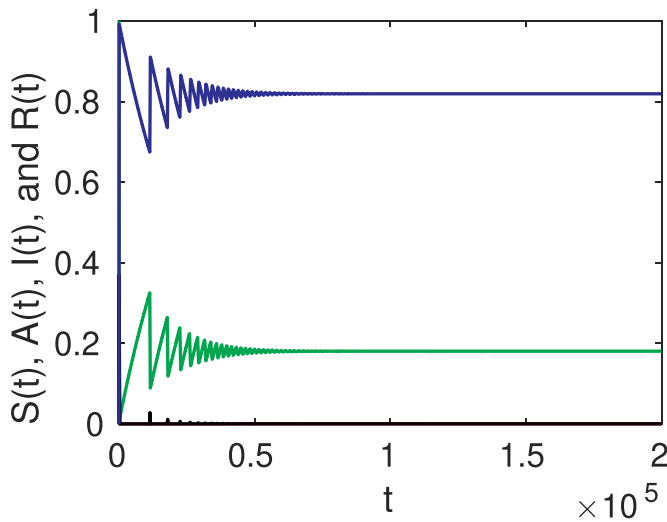


**Fig. 5.** Time evolutions of  $S(t)$  (green line),  $A(t)$  (black line),  $I(t)$  (red line), and  $R(t)$  (blue line) by using the same parameter values as employed in Fig. 4 and a larger time interval of the simulation. After an oscillatory transient, the system reaches an endemic steady-state given by  $S_2^* \approx 0.18$ ,  $A_2^* \approx 0.00020$ ,  $I_2^* \approx 0.00011$ , and  $R_2^* \approx 0.82$ . As in Fig. 2, the disease persists. (For interpretation of the references to color in this figure legend, the reader is referred to the web version of this article.)

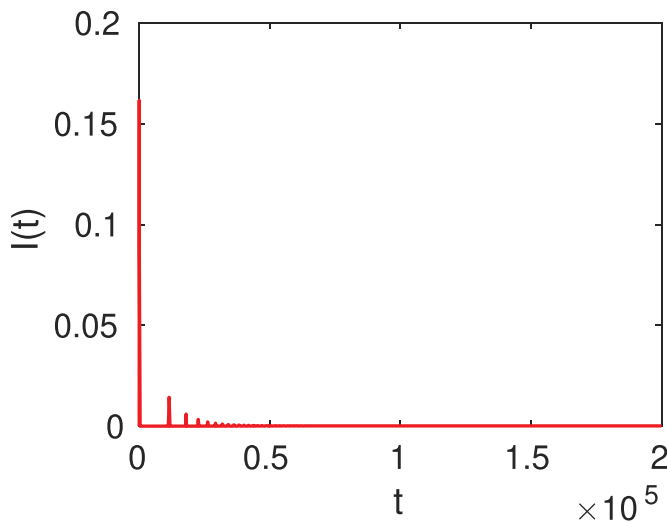


**Fig. 6.** Time evolution of  $I(t)$  presented in Fig. 5.

state; however, this convergence is faster and smoother as compared to Figs. 1–6.

#### 4. Discussion and conclusion

Usually, the COVID-19 propagation is theoretically investigated by considering  $E$ -individuals, which are those who were exposed to the pathogen and are in the incubation (latent) period of the infection (Gostic et al., 2020; Yang and Wang, 2020; Zhou et al., 2020). Such individuals, however, will become either asymptomatic or symptomatic, which are respectively the states  $A$  and  $I$  of the SAIR model proposed in this work. In this model, the four possible transmission pathways involving  $A$  and  $I$ -individuals are explicitly taken into account. The actual values of the corresponding rate constants ( $a_1, a_2, \alpha_1, \alpha_2$ ) of these pathways can be estimated from real-world data collected from contact tracing and screening programs for SARS-CoV-2. Limiting social contacts can decrease the values of these contagion parameters (Lai et al., 2020; Tang et al., 2020) and, consequently, the basic

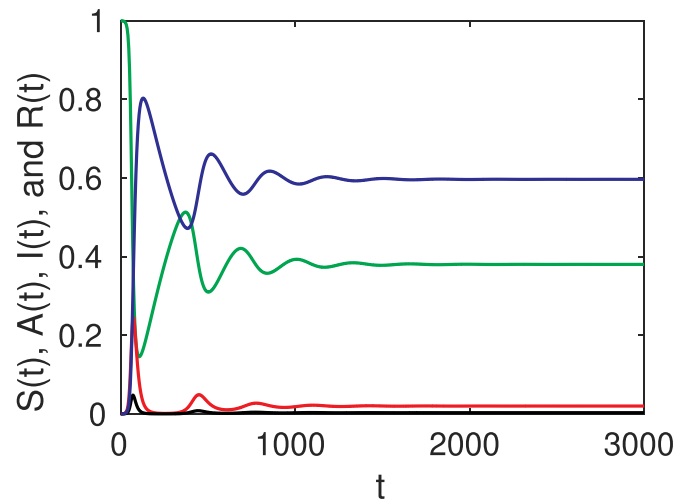


**Fig. 7.** Time evolutions of  $S(t)$  (green line),  $A(t)$  (black line),  $I(t)$  (red line), and  $R(t)$  (blue line) from  $S(0) = 99.99\%$ ,  $A(0) = 0.001\%$ ,  $I(0) = 0.009\%$ , and  $R(0) = 0\%$  obtained from the numerical integration of Eqs. (1)–(4) for  $N = 1$  and  $0 \leq t \leq 3000$ . In this simulation, the parameter values are  $a_1 = 0.01$ ,  $a_2 = 0.1$ ,  $\alpha_1 = 0.2$ ,  $\alpha_2 = 0.5$ ,  $b = 1/15$ ,  $\beta = 1/10$ ,  $c = 3/(100 \times 20)$ ,  $\gamma = 1/(365 \times 80)$ ,  $d = [1/(365 \times 80)] + (1/365)$ . In this figure, the convergence to the endemic steady-state is faster and smoother as compared to Fig. 1. (For interpretation of the references to color in this figure legend, the reader is referred to the web version of this article.)

reproduction number  $R_0$ . This control strategy has been implemented in many countries to reduce the transmission risk.

From the proposed model, formulas were derived for  $R_0$  (Eq. (16)), the endemic steady-state ( $S_2^*, A_2^*, I_2^*$ ) (Eq. (9)), the proportion  $q = I_2^*/A_2^*$  (Eq. (13)), and the stability of the disease-free steady-state (Eqs. (14) and (15)). These expressions can be employed to evaluate the effects of public health actions on the disease spread.

In the early phase of this pandemic, studies estimated  $R_0 \approx 2 - 6$ . Also, from the current knowledge of this illness,  $q \approx 0.25 - 9$ . From assumed values for the contagion rate constants  $a_1, a_2, \alpha_1$ , and  $\alpha_2$ , computer simulations were performed. Figs. 1–7 illustrate the results of three simulations. In Figs. 1–3 and 7,  $R_0 \approx 2.6$  and  $q \approx 6.3$ ; in Figs. 4–6,  $R_0 \approx 5.5$  and  $q \approx 0.54$ , which are acceptable values for  $R_0$  and  $q$ . Figs. 1–7 show that the viral infection is not naturally eradicated after the first peak. In fact, there is a sustained transmission after an oscillatory transient. This transient implies that, from times to times, peaks in the amount of sick individuals can occur.

It is relevant to stress that the proportion of the infected population in steady state, given by  $A_2^* + I_2^*$ , can be very very small. In fact, from Eqs. (5)–(7), the following relation can be obtained:

$$S_2^* = 1 - \left[ \frac{(\beta + d)A_2^* + (b + d)I_2^*}{d} \right] \tag{17}$$

by taking  $N = 1$ . For the vast majority of viral infections,  $\beta \gg d$  and  $b \gg d$ , because the recovery time (typically, one or two weeks) is much shorter than the duration of acquired immunity (typically, years or decades) and the average life expectancy (typically, six to eight decades, depending on the country). Therefore:

$$S_2^* \approx 1 - \left[ \frac{\beta A_2^* + b I_2^*}{d} \right] = 1 - R_2^* \tag{18}$$

or:

$$S_2^* + R_2^* \approx 1 \tag{19}$$

Thus, in steady state, the population is composed almost exclusively of  $S$  and  $R$ -individuals. For instance, for the simulations shown in Figs. 1–6,  $A_2^* + I_2^* \approx 0.0003$ ; in Fig. 7,  $A_2^* + I_2^* \approx 0.024$ . Depending on the parameter values,  $A(t) + I(t)$  can also be very very small between

two consecutive peaks. In practice, too small numbers can correspond to eradication. For instance, if  $A(t') + I(t') = 0.00001$  at a given instant  $t'$  and the host population is composed of 10000 individuals (a small city), then the number of sick individuals at the instant  $t = t'$  is  $10000 \times 0.00001 = 0.1$ . In practice, the disease is eradicated (because the number of individuals must be a positive integer number). Obviously, local eradication (in small cities) do not imply global eradication (in big cities or countries) (Bartlett, 1957; Monteiro et al., 2006).

A final remark: the spread of SARS-CoV (severe acute respiratory syndrome coronavirus) was halted, but the spread of MERS-CoV (Middle East respiratory syndrome coronavirus MERS-CoV) still continues (Song et al., 2020). The fate of SARS-CoV-2, the third highly pathogenic coronavirus emerging in two decades, remains unclear. However, notice that it can persist and/or be reintroduced in our population due to the interaction with environmental reservoirs. Therefore, without preventive attitudes (such as improved hygiene habits, movement restrictions, social distancing, wearing face masks) and in the absence of vaccine for inducing an immune response and of approved drugs for treating patients, an endemic persistence can be the future of COVID-19.

#### CRediT authorship contribution statement

**L.H.A. Monteiro:** Conceptualization, Methodology, Software, Validation, Formal analysis, Investigation, Resources, Data curation, Writing - original draft, Writing - review & editing, Visualization, Supervision, Project administration, Funding acquisition.

#### Declaration of Competing Interest

The authors declare that they have no known competing financial interests or personal relationships that could have appeared to influence the work reported in this paper.

#### Acknowledgments

LHAM is partially supported by Conselho Nacional de Desenvolvimento Científico e Tecnológico (CNPq) under the grant #304081/2018-3. This study was financed in part by the Coordenação de Aperfeiçoamento de Pessoal de Nível Superior (CAPES) - finance code 001.

#### References

- Anderson, R.M., May, R.M., 1992. *Infectious Diseases of Humans: Dynamics and Control*. Oxford University Press, Oxford.
- Bartlett, M.S., 1957. Measles periodicity and community size. *J. R. Stat. Soc. Ser. A* 120,

- 48–70.
- Day, M., 2020a. COVID-19: four fifths of cases are asymptomatic, China figures indicate. *BMJ-Brit. Med. J.* 369, M1375.
- Day, M., 2020b. COVID-19: identifying and isolating asymptomatic people helped eliminate virus in Italian village. *BMJ-Brit. Med. J.* 368, M1165.
- Diekmann, O., Heesterbeek, J.A.P., Roberts, M.G., 2010. The construction of next-generation matrices for compartmental epidemic models. *J. R. Soc. Interface* 7, 873–885.
- van den Driessche, P., 2017. Reproduction numbers of infectious disease models. *Infect. Dis. Model.* 2, 288–303.
- Ferraz, D.F., Monteiro, L.H.A., 2019. The impact of imported cases on the persistence of contagious diseases. *Ecol. Complex.* 40 (100788), 1–4.
- Fitch, J.P., 2015. Engineering a global response to infectious diseases. *Proc. IEEE* 103, 263–272.
- Gostic, K., Gomez, A.C.R., Mummah, R.O., Kucharski, A.J., Lloyd-Smith, J.O., 2020. Estimated effectiveness of symptom and risk screening to prevent the spread of COVID-19, 2020. *eLife* 9 (e55570), 1–18.
- Guckenheimer, J., Holmes, P., 2002. *Nonlinear Oscillations, Dynamical Systems, and Bifurcations of Vector Fields*. Springer, New York.
- Hu, Z.L., Song, C., Xu, C.J., Jin, G.F., Chen, Y.L., Xu, X., Ma, H.X., Chen, W., Lin, Y., Zheng, Y.S., Wang, J.M., Hu, Z.B., Yi, Y.X., Shen, H.B., 2020. Clinical characteristics of 24 asymptomatic infections with COVID-19 screened among close contacts in Nanjing, China. *Sci. China-Life Sci.* <https://doi.org/10.1007/s11427-020-1661-4>. (in press).
- Kretzschmar, M., 2019. Disease modeling for public health: added value, challenges, and institutional constraints. *J. Public Health Policy* 41, 39–51.
- Lai, C.C., Shih, T.P., Ko, W.C., Tang, H.J., Hsueh, P.R., 2020. Severe acute respiratory syndrome coronavirus 2 (SARS-cov-2) and coronavirus disease-2019 (COVID-19): the epidemic and the challenges. *Int. J. Antimicrob. Agents* 55 (105924), 1–9.
- Mizumoto, K., Kagaya, K., Zarebski, A., Chowell, G., 2020. Estimating the asymptomatic proportion of coronavirus disease 2019 (COVID-19) cases on board the Diamond Princess cruise ship, Yokohama, Japan. *Eurosurveillance* 25. 2000180/2-6.
- Monteiro, L.H.A., Chimara, H.D.B., Chaui Berlinck, J.G., 2006. Big cities: shelters for contagious diseases. *Ecol. Model.* 197, 258–262.
- Pennekamp, F., Adamson, M.W., Petchey, O.L., Poggiale, J.C., Aguiar, M., Kooi, B.W., Botkin, D.B., DeAngelis, D.L., 2017. The practice of prediction: what can ecologists learn from applied, ecology-related fields? *Ecol. Complex.* 32, 156–167.
- Schimit, P.H.T., Monteiro, L.H.A., 2010. Who should wear mask against airborne infections? Altering the contact network for controlling the spread of contagious diseases. *Ecol. Model.* 221, 1329–1332.
- Singhal, T., 2020. A review of coronavirus disease-2019 (COVID-19). *Indian J. Pediatr.* 87, 281–286.
- Song, Z.Q., Xu, Y.F., Bao, L.L., Zhang, L., Yu, P., Qu, Y.J., Zhu, H., Zhao, W.J., Han, Y.L., Qin, C., 2020. From SARS to MERS, thrusting coronaviruses into the spotlight. *Viruses-Basel* 11, 59.
- Tang, B., Wang, X., Li, Q., Bragazzi, N.L., Tang, S.Y., Xiao, Y.N., Wu, J.H., 2020. Estimation of the transmission risk of the 2019-nCoV and its implication for public health interventions. *J. Clin. Med.* 9 (462), 1–13.
- Turnes Jr., P.P., Monteiro, L.H.A., 2014. An epidemic model to evaluate the homogeneous mixing assumption. *Commun. Nonlinear Sci. Numer. Simul.* 19, 4042–4047.
- Velavan, T.P., Meyer, C.G., 2020. The COVID-19 epidemic. *Trop. Med. Int. Health* 25, 278–280.
- Wu, J.T., Leung, K., Bushman, M., Kishore, N., Niehus, R., deSalazar, P.M., Cowling, B.J., Lipsitch, M., Leung, G.M., 2020. Estimating clinical severity of COVID-19 from the transmission dynamics in Wuhan, China. *Nat. Med.* <https://doi.org/10.1038/s41591-020-0822-7>. (in press).
- Yang, C.Y., Wang, J., 2020. A mathematical model for the novel coronavirus epidemic in Wuhan, China. *Math. Biosci. Eng.* 17, 2708–2724.
- Zhou, W.K., Wang, A.L., Xia, F., Xiao, Y.N., Tang, S.Y., 2020. Effects of media reporting on mitigating spread of COVID-19 in the early phase of the outbreak. *Math. Biosci. Eng.* 17, 2693–2707.